Free Liquid Piston Ericsson Engine: Dynamic Modelling and Experimental Validation

Victor LANCELEUR [a], Nicolas JOBERT [b], Pascal STOUFFS [c] and Sébastien THOMAS [d]

[a] Extrajool & LaTEP, Pau, France, victor.lanceleur@univ-pau.fr
[b] Alma Consulting Precision Engineering Services, Paris, France, nicolas.jobert@alma-consulting.eu,
[c] Universite de Pau et des Pays de l'Adour, LaTEP, Pau, France, pascal.stouffs@univ-pau.fr,
[d] ExtraJool, Bordeaux, France, sebastien.thomas@extrajool.com

Abstract:

This study presents the development and validation of a numerical program for the analysis of an external heat supply engine, with a particular focus on its dynamic behavior. The engine in question is a Free Liquid Piston Ericsson engine, based on an open-air Joule cycle. The numerical model was designed to predict this specific engine's operating characteristics under controlled conditions and was systematically compared against an experimental counterpart developed for the same configuration. The model's versatility also allows for its application in approaching new complex designs using multiple cylinders. Correlation between numerical and experimental results was assessed using both qualitative and quantitative approaches. Qualitative validation was achieved through direct comparison of the temporal evolution and trends observed in the numerical and experimental response curves, showing consistent behavior across operating cycles. Quantitative validation was performed by measuring multiple indicators such as the piston end-stroke displacement in both environments, allowing for a direct and physically meaningful comparison. The results demonstrate a strong agreement between the numerical predictions and experimental measurements, with only minor deviations attributable to experimental uncertainties and modeling assumptions. These findings confirm the reliability of the numerical program as a predictive and design-support tool and highlight its potential for further optimization and performance analysis of external heat supply engines.

Keywords:

Free liquid piston; Ericsson engine; Dynamic modelling; External heat supply engine; Experimental validation.

1. Introduction

Growing interest in sustainable and fuel-flexible power generation has renewed attention toward reciprocating engines with external heat supply, which offer advantages such as reduced emissions, and improved thermal management [1]. Among these technologies, Ericsson engines based on a theoretical Joule cycle represent a promising alternative due to their theoretical efficiency and compatibility with external heat sources [2-8].

Free piston engines have been extensively studied in recent decades [9,10] because they eliminate the crankshaft mechanism, thereby reducing mechanical losses and allowing greater operational flexibility. In particular, in Free Liquid Piston compressors or expanders the solid piston is replaced with a liquid column, enabling friction reduction, self-adaptive stroke length, and simplified sealing [11,12]. When combined with an open-air Joule cycle, this configuration becomes especially attractive for low-grade heat recovery and distributed energy systems [13,14].

Despite these advantages, the dynamic behavior of free liquid piston systems remains complex. The absence of a kinematic constraint introduces strong coupling between thermodynamic processes and piston motion, making accurate modelling essential. While several numerical approaches have been proposed for free piston engines, limited work has addressed liquid piston Ericsson engines with experimental validation under realistic operating conditions [15].

The objective of this study is therefore twofold:

1. To develop a dynamic numerical model capable of accurately predicting the behavior of a Free Liquid Piston Ericsson engine.

2. To validate the model through systematic comparison with experimental data obtained from dedicated tests benches.

The validated numerical program is intended not only as an analysis tool but also as a foundation for future optimization studies and multi-cylinder engine designs.

2. Engine Configuration and Operating Principles

2.1. Free Liquid Piston Ericsson Engine Concept

The investigated engine operates according to an open-air Joule (Ericsson) cycle with external heat addition. The working fluid is ambient air, which undergoes compression, heating, expansion, and exhaust processes.

In contrast to conventional piston engines, the FLPEE employs a liquid piston, typically water or special liquid compound [12], contained within a vertical cylinder. The liquid column acts as both a piston and a sealing medium, separating the working gas from the mechanical boundary. The piston motion is governed by pressure differences across the liquid column and by gravitational and inertial effects. Figure 1 illustrates the general principle of the system. An open recuperated Joule cycle is considered with air as the working fluid. The left-hand side of the U column acts as the compressor, while the expansion is carried out in two parts, the first one in the right-hand side of the U column, to provide the mechanical energy needed for the compression, the second one in an external expander to provide the useful mechanical energy. In this configuration, the liquid piston system act as a compressed air generator.

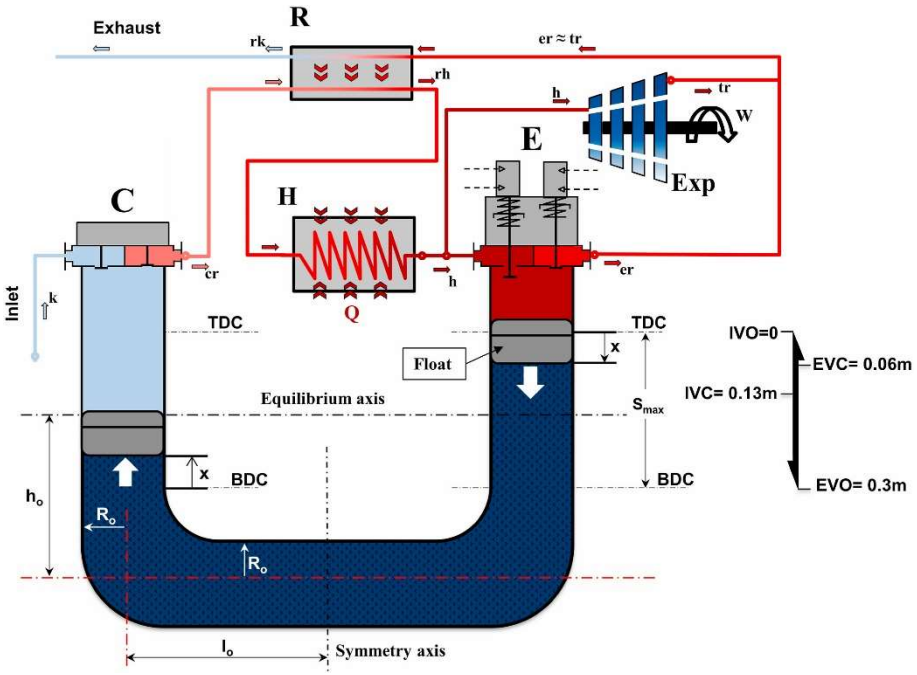

Figure 1. *Liquid piston Ericson engine [3]*

2.2. Experimental Prototype

2.2.1. Prototype Overview

The experimental engine consists of:

- Both compression & expansion cylinder partially filled with liquid
- An external heat exchanger supplying controlled thermal input
- Inlet and exhaust controlled and check valves regulating the open-cycle operation
- Sensors for pressure, temperature, and piston displacement

Liquid piston motion is free, with no mechanical linkage imposing a predefined stroke, allowing the system to reach a natural dynamic equilibrium under given boundary conditions.

Two prototypes have been used for experimental validation of the numerical model. Figure 2 shows the first small U-tube prototype.

Figure 2. *Small prototype overview*

Figure 3 shows the same prototype equipped with heat exchangers. The expansion branch of the U-tube is clearly seen in the foreground, together with the electrical hot source heat exchanger and several temperature and pressure sensors.

Figure 3. *Small prototype overview, focus on the expansion cylinder*

Figure 4 presents another view of the small prototype with the buffer tank for compressed air between the compressor branch and the expansion branch of the U-tube in the foreground.

Figure 4. *Small prototype overview, focus on the buffer tank*

A larger W-tube liquid piston prototype has also been used for model validation.

2.2.2. Experimental Methodology

The validation of the numerical model was carried out through a systematic comparison between experimental measurements and simulation results. The objective of this methodology was to evaluate the ability of the model to reproduce the thermodynamic and dynamic behavior of the engine under a range of operating conditions. Experiments were performed on a prototype based on the Ericsson cycle, for which several configurations and operating parameters were investigated.

First, **different engine designs** were considered in order to assess the sensitivity of the model to geometrical parameters and system architecture. These configurations mainly involved variations in characteristic dimensions and internal volumes that influence the compression and expansion processes. For each configuration, a corresponding numerical setup was implemented so that the geometrical and physical parameters of the simulation matched those of the experimental prototype as closely as possible.

The experiments were then conducted for **several working pressures** of the engine, typically ranging from about 1.4 to 2 bar absolute pressure. Adjusting the mean pressure level allowed the study of its influence on the thermodynamic behavior of the system. For each selected pressure level, the engine was operated until stable cyclic conditions were reached, and the relevant variables were recorded.

In addition, **distinct operating cycles** of the engine were investigated. These cycles correspond to different operating regimes that affect the timing of gas exchange processes, the amplitude of pressure variations, and the overall dynamic response of the system. The numerical model was run under the same conditions as the experiments, using identical initial and boundary conditions whenever possible.

2.2.3. Experimental equipment

During this experimental research, a dashboard was developed that functions as an integral component of the data acquisition and validation pipeline rather than a simple visualization tool (Figure 5). It provides real-time structuring and display of incoming data, enabling immediate detection of anomalies such as noise, target drift, or measurement inconsistencies. This significantly reduces data loss and limits the need for repeated experiments, which was becoming an impactful issue with more than 20 experiments a week.

A central feature of the system is the integration of metadata with raw measurements. By linking each data point to acquisition parameters (e.g., instrument settings, calibration, timing), the dashboard ensures traceability and supports continuous validation of experimental conditions. This transforms it into an active monitoring environment where data quality can be assessed as measurements are produced. The dashboard also standardizes data representation and allows real-time transformations such as filtering or normalization without altering raw data. This supports on-the-fly analysis and rapid hypothesis testing, shortening the feedback loop between observation and experimental adjustment.

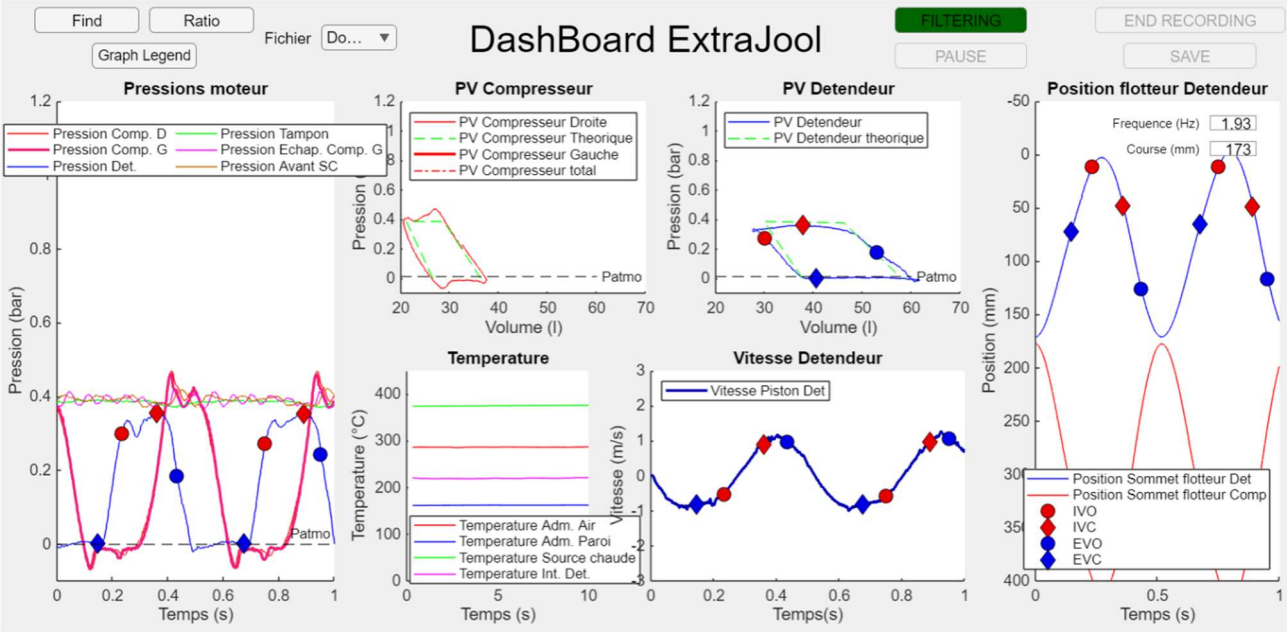

***Figure 5**. Dashboard used for ExtraJool engine experiments*

3. Numerical modelling

3.1. Modelling approach

A time-dependent numerical model was developed to simulate the coupled thermodynamic and dynamic behavior of the engine during its operation. It incorporates the **mass and energy balance equations** describing the thermodynamic evolution of the working gas, while also including the **momentum balance** governing the motion of the liquid piston [6]. In addition to these fundamental balances, the model represents the heat transfer exchanged between the cylinders, which plays an important role in determining the thermal performance of the system. The dynamics of the inlet and exhaust valves are also considered through a formulation of the valve flow behavior during the gas exchange processes. All these coupled equations are solved using a time-stepping numerical approach, enabling the simulation to capture the transient evolution of the system until it reaches the establishment of cyclic steady-state operating conditions.

3.2. Governing equations

Two core equations allow to have a better understanding of the engine dynamics.

First one being the piston motion, which is governed by a dynamic force balance:

$$m_l \vec{a} = \vec{F}_P + \vec{P} + \vec{F}_{loss}$$

where ($\vec{P}$) is the liquid's weight, (a) its acceleration, ($\vec{F}_P$) the difference of gas pressure force between the cylinder, and ($\vec{F}_{loss}$) represents viscous and hydraulic losses. In a numerical simulation framework, this formulation is particularly useful because it naturally fits within a time-stepping approach. Instead of relying on a fully analytical formulation involving general derivatives of position with respect to time, the acceleration obtained from the force balance can be integrated step by step over small time increments to update the velocity and position of the system.

In order to simulate a coherent pressure force, we describe the mass airflow through the intake and exhaust components via the formulation derived from the Saint-Venant–Wantzel equation, which originates from the compressible flow theory developed by Adhémar Jean Claude Barré de Saint-Venant and Valentin Wantzel. This relation is used to estimate the mass flow rate of a compressible gas passing through an orifice, valve, or nozzle when a pressure difference exists between two reservoirs. In the context of the engine model, the equation provides a physically consistent way to describe the gas exchange processes occurring at the inlet and exhaust valves. The flow rate is determined as a function of the upstream pressure and temperature, the downstream pressure, and the effective flow area of the valve. Because air behaves as a compressible fluid under these conditions, the formulation also accounts for the possibility of choked flow, which occurs when the pressure ratio between the upstream and downstream sides reaches a critical value and the flow velocity at the restriction approaches the speed of sound.

Within the time-stepping numerical framework, the Saint-Venant–Wantzel relation is evaluated at each time step using the instantaneous thermodynamic conditions in the engine chamber and in the intake or exhaust reservoir. This allows the model to dynamically update the mass flow rate entering or leaving the system as pressures and temperatures evolve during the cycle.

$$\dot{m} = AC_d p \left[\frac{2\gamma}{(\gamma - 1)rT} \left(R^{\frac{2}{\gamma}} - R^{\frac{\gamma+1}{\gamma}} \right) \right]^{\frac{1}{2}}$$

3.3. Model assumptions

The numerical model key assumptions include:

- **A one-dimensional piston motion:** By allowing only one degree of movement to focus solely on the downward/upward force, which is the path of least resistance, and neglecting the lateral vectors of the compressed liquid.
- **A uniform gas property:** Within the cylinder, the difference of velocity between moving piston and the speed of sound for air displacement allows for a homogeneous gas repartition at any given time.
- **Adiabatic Cylinder:** In the present model, the thermodynamic process of working gas is assumed to be nearly **adiabatic**. This assumption is justified by the relatively low heat transfer coefficient between the air and the stainless-steel surfaces that form the boundaries of the chamber. It results in relatively weak heat transfer during the short time scale of the compression and expansion processes.
- **Incompressible liquid:** As for the liquid piston, it is important that it remains incompressible to further justify its advantages, even during transitory flow state.
- **The opening delay** for admission and exhaust of both controlled and check valves are to be constant.

These assumptions were selected to balance model accuracy and computational efficiency.

3.4. Model validation

3.4.1. Qualitative validation

The comparison between the experimental results and the numerical simulation shows a generally remarkable consistent trend between both datasets, indicating that the numerical model successfully captures the main behavior of the system (Figure).

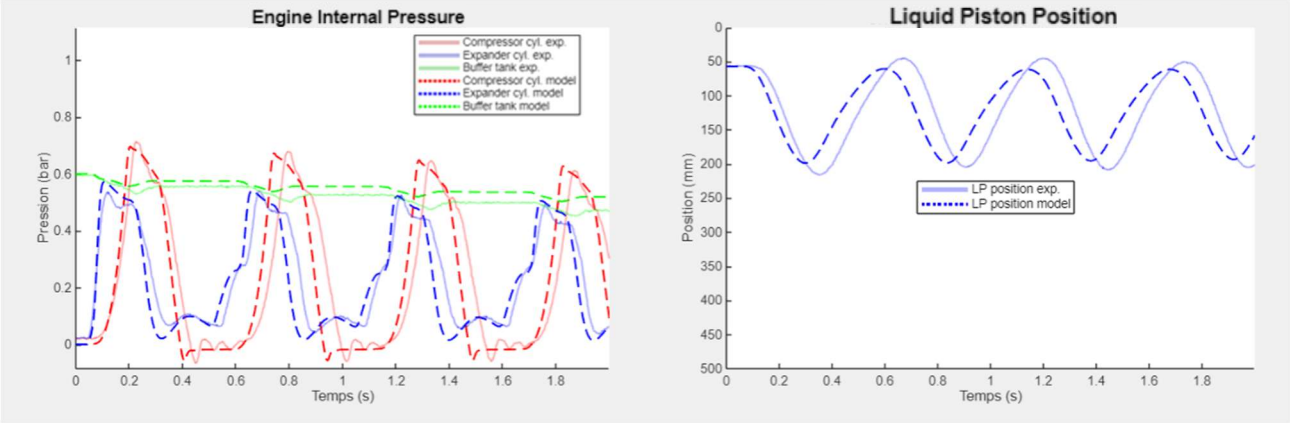

Figure 6. *Comparison between experiment (solid line) and the numerical model (dashed line)*

From a qualitative perspective, the overall **shape and progression of the curves** in the numerical graph closely follow those obtained experimentally. Both graphs display similar patterns during the major stages of the Ericsson cycle, particularly during the **isentropic compression and expansion processes** characteristic of the Ericsson Cycle. This similarity suggests that the assumptions used in the computational model adequately represent the fundamental physics governing engine operation.

When examining the graph, the **trend alignment** between the two datasets is evident. As the characteristic parameters (such as pressure, chamber volume or piston position) change throughout the cycle, the numerical model reproduces the same behavior observed experimentally. For example in **Figure** , during the expansion phase of the expander cylinder, illustrated by the piston moving downward (*position axis is inverted as a consequence of choosing the cylinder head as position of reference*) while pressure drop to atmospheric in the expander and rise up to working pressure in the compressor, both the experimental and numerical curves exhibit a comparable decrease of position and pressure variation. On top of an identical frequency, this indicate that the simulation correctly predicts the thermodynamic response of the system.

However, a single comparison alone cannot validate the full extent of the numerical model. Based on the methodology detailed above, numerous examples of comparisons between experimental and numerical results are presented in Figure 7.

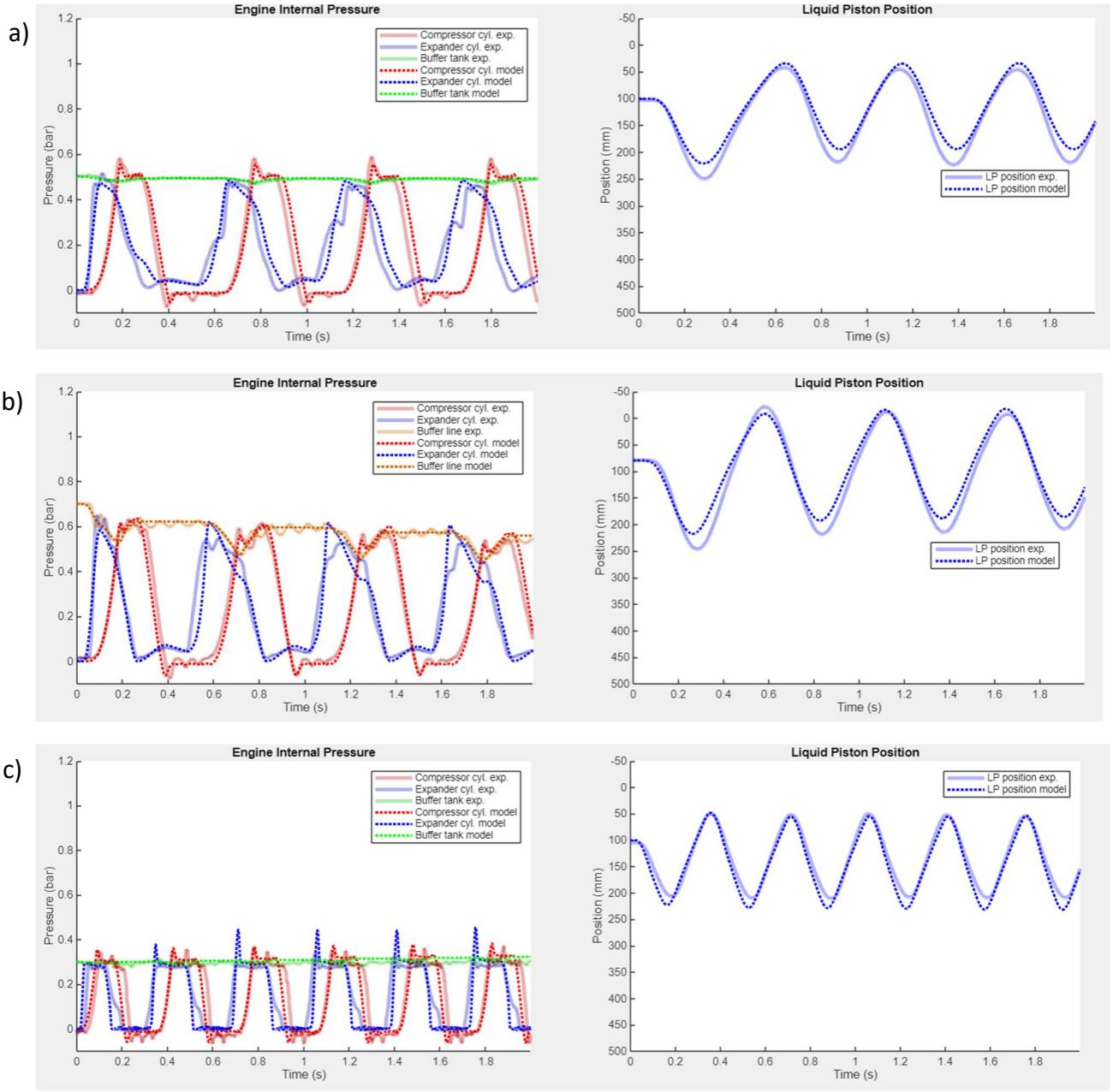

Figure 7. *Comparison between experiment and model: a) W-engine's hot-running operation, b) Higher pressure and removal of floater, c) U-Engine smaller dimension*

Each sub-figure of Figure 7 represents a unique comparison between experimental and numerical results pointing toward the good behavior of the simulation while varying several parameters such as geometrical size, operational pressure or temperature. **Figure** .a) displays one of the first test on the W-engine using a heat exchanger with temperature reaching up to 250°C. A gap between the experimental and numerical position of the liquid piston can be seen when the liquid piston reaches its lower position value. Thanks to the model, this was later explained as follows. Actually, the liquid piston position is measured by lidar detecting the position of the float at the water surface. However, at the end of the liquid piston's downward stroke, the floating device sinks slightly due to inertia. This test will be the reference, for the purpose of staying coherent when changing relevant parameters.

Figure .b) explores the same W-engine design while modifying key parameters such as floater removal, increase of water level, decrease of working temperature, higher air pressure and even reducing drastically the buffer volume. By accounting for all of these changes and only these changes, the model can **accurately** replicate the on-site data, as seen on the buffer line conduct.

Lastly, **Figure** .c) experience takes place with the very first U-engine shape that was used for the core of the model. A much higher frequency can be observed with stroke length fairly close to the ones of the previous figure. However, the real distinction lies behind the hidden parameter, which are the total air volume displaced (10 times lower) and the water quantity in the liquid piston that plays a big role in the liquid piston dynamic.

In all these comparisons between experimental and numerical results, some discrepancies may appear, such as **small shifts in peak values, slight offsets in magnitude, or differences in the steepness of the curves**. Such small differences can probably be explained by factors such as **heat losses, fluid turbulence, measurement uncertainty, and imperfect boundary conditions**.

3.4.2. Quantitative validation

The purpose of this approach is to isolate particular test cases from the experimental campaign and directly compare them with the corresponding results obtained from the numerical simulation. By focusing on individual properties such as piston oscillation, rate of pressure increase or stroke length, it becomes possible to evaluate how accurately the model predicts key thermodynamic variables in periodic steady states.

For each selected unit test presented in Table 1, the numerical values predicted by the model are compared with the experimentally measured data. The difference between the two values is then evaluated through quantitative indicators such as **absolute error, relative error, or percentage deviation**. This process allows the degree of agreement between the numerical model and the experimental results to be assessed in a more objective and measurable manner.

The results obtained from the unit tests generally show that the numerical predictions remain within an acceptable deviation range compared to the experimental measurements.

Table 1. Unit tests used to assess the model's accuracy

Label	Description	Purpose
TUS1	**Open cylinder heads, free oscillation**	**Verification of gravity effect**
TUS2	Closed cylinder heads, free oscillations	Verification of gas spring effect
TUS3	Same as TUS2, with dry friction	Finite response time
TUS4	Same as TUS2, with viscous friction	Exponential decay
TUS5	Same as TUS2, with turbulent friction	Power dissipated per cycle
TUS11	Heating of the buffer tank	Temperature rise, discharge flow
TUS12a/b	**Depressurization of the buffer tank through the discharge valve**	**Adiabatic / isothermal emptying**
TUS13	Expansion of the buffer tank into the discharge valve	Verification of isothermal expansion
TUS21	Closed valves, free response with generator	Mechanical power delivered

For instance, Figure 8 presents the experimental results corresponding to unit test TUS1. In Figure , both graphs show a very similar dynamic behavior of the liquid piston, seen as such on experimental data (a) compared to the numerical model (b). In both cases, the motion is clearly oscillatory (the left graph represent only the highest point of the liquid surface), with the liquid column moving up and down over time due to pressure variations in a U-shaped conduit. A key similarity is the presence of damping: the amplitude of the oscillations decreases progressively in both graphs, indicating energy losses (likely due to viscous effects and friction). Additionally, the estimated frequencies are close (around 0.7–0.8 Hz), which suggests that the model captures the natural oscillation rate of the real system quite well with the last points recorded after 30s being at the same height.

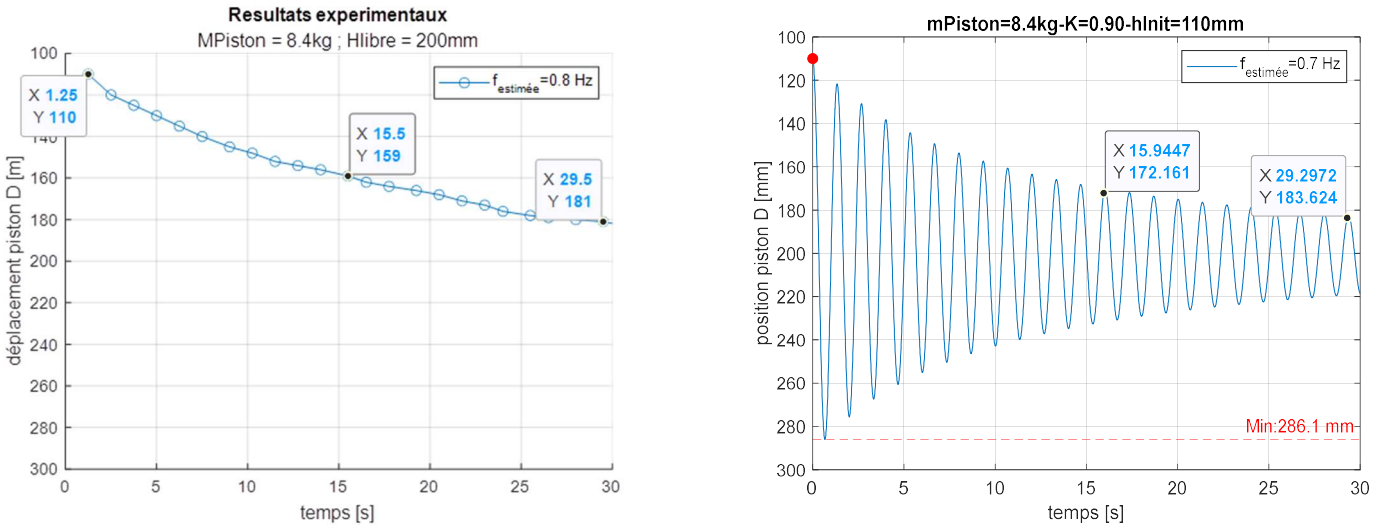

a) b)

Figure 8. *Open cylinder heads, free oscillation: a) observed through semi-transparent cylinder, b) simulated through the model behavior*

Figure 9 presents the results corresponding to unit test TUS12a.

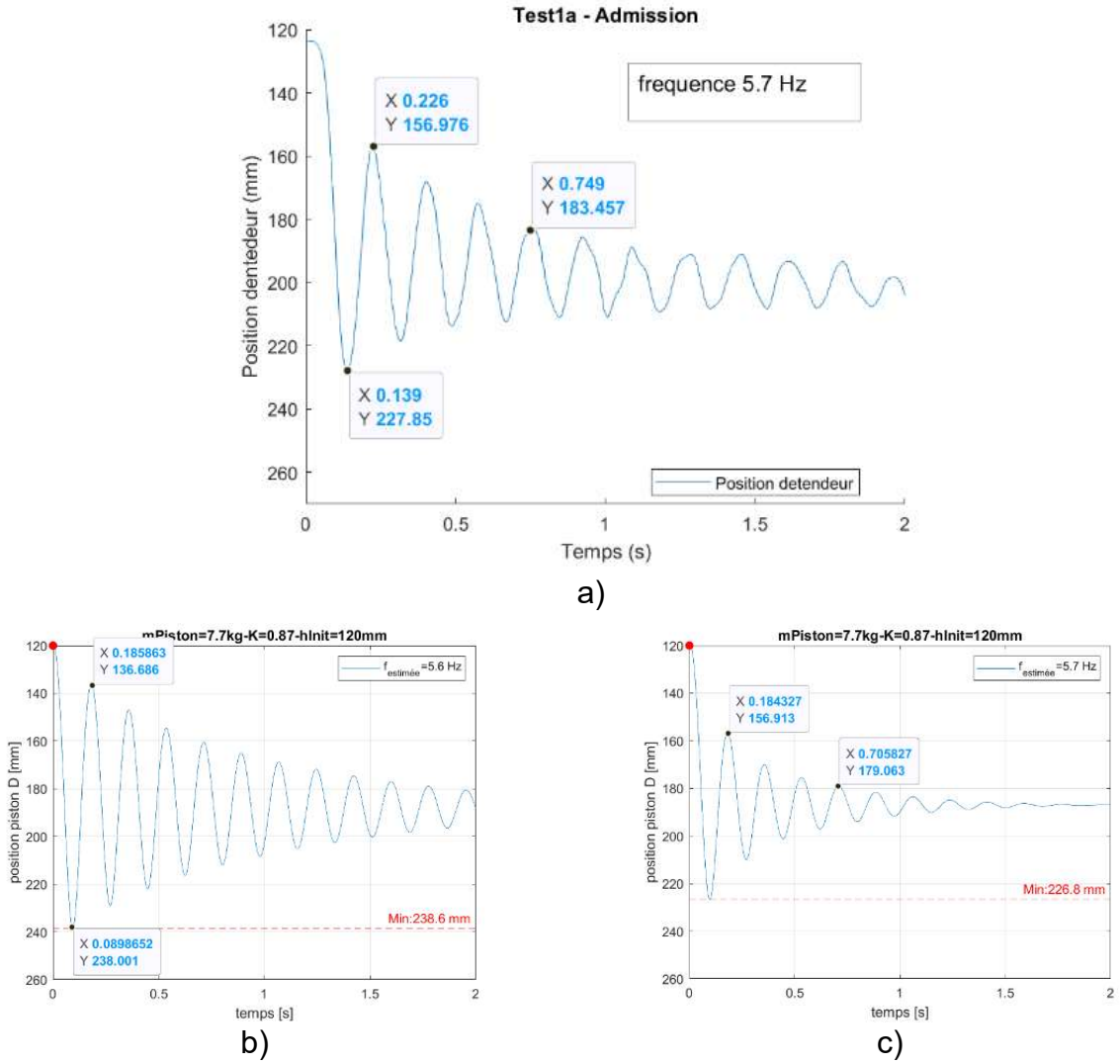

a) b) c)

Figure 9. *Depressurization of the buffer tank through the discharge valve: a) Experiment result, b) Model solution with dry friction coefficient = 0.5, c) Model solution with dry friction coefficient = 1*

All three graphs on Figure exhibit the same fundamental physical behavior: a pressure discharge in one branch of the U-shaped conduit that induces oscillations of the liquid column. In each case, the system

responds with a periodic motion characterized by successive peaks and troughs, reflecting the conversion between pressure energy and fluid motion. As in the previous figure, the presence of damping is observed. The oscillations gradually decrease in amplitude over time, showing that energy is dissipated through mechanisms such as viscous friction, dry friction and flow resistance. The differences depicted in the graphs b) and c) right occurs because of a change in dry friction in the model.

4. Discussion

An important advantage of the developed numerical program is its modular structure, which allows extension to complex-cylinder configurations. Many parameters used in the numerical model are not explicitly listed in this article; however, they remain easily adjustable within the model framework. The model was intentionally designed to allow a high degree of flexibility so that different engine configurations can be evaluated without requiring significant modifications to the code or structure of the simulation. For instance, key geometric parameters such as the **number of cylinders** and their **dimensions** can be modified to study the impact of different engine layouts. In addition, the properties of the working liquid can be readily adjusted. Parameters like **volumetric mass, and viscosity** can be altered in order to analyze how different liquid characteristics influence the behavior of the system. Similarly, the thermodynamic properties of the gas phase can also be modified, enabling the model to simulate gases other than ambient air to evaluate their effect on engine performance.

5. Conclusion

Despite the small variations in both quantitative and qualitative assessment, the numerical results remain **reasonably close to the experimental data**, indicating that the computational model provides a reliable approximation of the engine behavior. It also exhibits **strong agreement in terms of general trend, cycle structure, and response behavior**, with only minor discrepancies likely caused by real-world inefficiencies and modeling simplifications. This level of agreement suggests that the numerical model is suitable for predicting the performance characteristics of the Ericsson liquid piston engine and can be used for further design optimization and performance analysis.

The numerical program is shown to be an effective predictive and design-support tool for external heat-supply engines and offers significant potential for future development of optimized liquid piston systems.

Acknowledgements

Victor Lanceleur thanks the French ‘Association Nationale de la Recherche et de la Technologie’ (ANRT) for its support and for providing the framework and funds that made this research possible.

References

[1] Finkelstein, T., Organ, A. J., 2001, Air engines, London: Professional Engineering Publishing Ltd.

[2] Komninos N. P., Rogdakis E. D., 2018, Design considerations for an Ericsson engine equipped with high-performance gas-to-gas compact heat exchanger: A numerical study, Appl. Therm. Eng., vol. 133, pp. 749–763, doi: 10.1016/j.applthermaleng.2018.01.078.

[3] Bell M. A., Partridge T., 2003, Thermodynamic design of a reciprocating Joule cycle engine, Proc Instn Mech Engrs Part A J Power Energy, vol. 217, pp. 239–246.

[4] Moss R. W., Roskilly A. P., Nanda S. K., 2005, Reciprocating Joule-cycle engine for domestic CHP systems, Appl. Energy, vol. 85, pp. 169–185.

[5] Creyx M., Delacourt E., Morin C., Desmet B., Peultier P., 2013, Energetic optimization of the performances of a hot air engine for micro-CHP systems working with a Joule or an Ericsson cycle, Energy, vol. 49, no. 1, pp. 229–239, 2013, doi: 10.1016/j.energy.2012.10.061.

[6] Stanciu D., Bădescu V., 2017, Solar-driven Joule cycle reciprocating Ericsson engines for small scale applications. From improper operation to high performance, Energy Convers. Manag., vol. 135, pp. 101–116, doi: 10.1016/j.enconman.2016.12.070.

[7] Touré, A., Stouffs, P., 2014, Modeling of the Ericsson engine, Energy, Volume 76, 1, p. 445-452.

[8] Ndamé Ngangué, M., Sosso Mayi, O., Stouffs, P., 2019, Study of three valves command laws of the expansion cylinder of a hot air engine, International Journal of Thermodynamics (IJoT), Vol. 22 (No. 2), pp. 84-96, doi: 10.5541/ijot.499621.

[9] Mikalsen, R., Roskilly, A.P., 2007, A review of free-piston engine history and applications, Appl. Therm. Eng., 27, 2339–2352, doi: 10.1016/j.applthermaleng.2007.03.015.

[10] Zare, S., Tavakolpour-Saleh, A.R, 2020, Free piston Stirling engines: A review, Int. J. Energy Research, 44, 5039–5070, doi: 10.1002/er.4533.

[11] Van De Ven, R. J. D., Li, P. Y., 2009, Liquid piston gas compression, Appl. Energy, 86 (2009), 2183–2191, doi: 10.1016/j.apenergy.2008.12.001.

[12] Specklin, M., Deligant, M., Sapin, P., Solis, M., Wagner, M., Markides, C. N., & Bakir, F. (2022). Numerical study of a liquid-piston compressor system for hydrogen applications. Applied Thermal Engineering, 1873-5606; DOI: 10.1016/j.applthermaleng.2022.118946.

[13] Ndamé Ngangué, M., Sosso Mayi, O., Stouffs, P., 2019, Dynamic simulation of an original Joule cycle liquid pistons hot air Ericsson engine. Energy, pp.116293. ⟨10.1016/j.energy.2019.116293⟩

[14] Chouder, R., Benabdesselam A., Stouffs, P., 2023, Modeling results of a new high performance free liquid piston engine, Energy, 263, 125960, doi:10.1016/j.energy.2022.125960.

[15] Chouder, R., Ndamé Ngangué, M., Stouffs, P., Benabdesselam, 2023, A., First experimental results of a new free liquid piston Ericsson engine, Proceedings of ECOS 2023, paper 1371.